Structural Variations and Formation Constants of First-Row Transition Metal Complexes of Biologically Active Aroylhydrazones

Claire M. Armstrong,[a] Paul V. Bernhardt,*[a] Piao Chin,[a] and Des R. Richardson[b]

Keywords: Hydrazones / Structure elucidation / Transition metals / N ligands

Iron chelators of the 2-pyridinecarbaldehyde isonicotinoylhydrazone (HPCIH) class show high potential for the treatment of iron overload diseases. In the present study, selected first-row transition metal (from Mn to Zn) complexes with HPCIH and 2-pyridinecarbaldehyde (4′-aminobenzoyl)hydrazone (HPCAH) were synthesised and characterised. Crystallography reveals that HPCAH exclusively forms bis complexes with divalent transition metals, with each ligand coordinating meridionally through its pyridine-N, imine-N and carbonyl-O atoms, forming distorted octahedral *cis*-MN_4O_2 complexes. Complexes of HPCIH were more varied and unpredictable, with metal/ligand ratios of 1:1, 1:2, 2:2 and 3:2 obtained with different metal ions. The isonicotinoyl ring N-atom in HPCIH was found to be an effective ligand, and this resulted in the varied metal/ligand ratios observed. The formation constants of divalent metal complexes with HPCIH were determined by potentiometric titrations and the values obtained were consistent with similar tridentate ligands and with the Irving–Williams order.

Introduction

In recent years the search for an orally effective drug for iron (Fe) overload diseases has gained increasing attention.[1−3] The motivating factors behind this interest are that the chelator in current clinical use, desferrioxamine B (DFO, see Scheme 1),[4] is expensive, is found to cause serious side effects in some patients, and is orally ineffective. In fact, DFO requires frequent and long periods of subcutaneous infusion leading to poor patient compliance.[5,6]

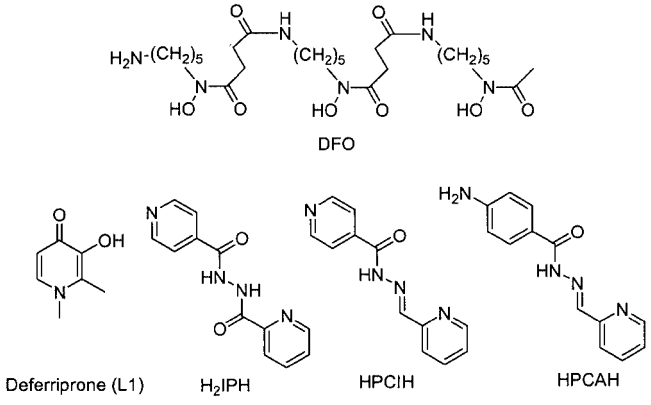

Scheme 1

An orally active alternative drug, deferiprone (also known as L1, see Scheme 1), was developed and extensively tested in the 1980s and 1990s,[7,8] but was found to result in myelotoxicity, liver fibrosis and have limited ability to reduce hepatic Fe levels.[9−11] Indeed, the use of this chelator remains controversial.[12] However, recent studies have shown more promise,[13−15] particularly when DFO is combined with Deferiprone.[16,17] Lipophilic Fe chelators have also been proposed for the treatment of other Fe-loading diseases such as the severe neurological disease Friedreich's ataxia.[18] If successful, this strategy will provide a new therapeutic application for these compounds.[18,19]

Our research program revolves around the design and synthesis of ligands that exhibit high Fe chelation efficacy and are potentially orally effective. We have designed and patented a novel class of ligands based on 2-pyridinecarbaldehyde isonicotinoylhydrazone (HPCIH, see Scheme 1), that have shown great promise in vitro, demonstrating a high Fe chelation efficacy.[20−22] Moreover, these chelators show very low toxicity in vitro in cultured cells and the compounds are simple and economical to prepare by a Schiff-base condensation reaction.[19−23]

Interestingly, and unexpectedly, the parent chelator of this class, HPCIH, has been shown to be oxidized by Fe^{III} to the diacylhydrazine, *N*-(isonicotinoyl)-*N*′-(picolinoyl)hydrazine (H_2IPH; see Scheme 1).[23] In contrast, in the absence of Fe^{III}, the parent hydrazone is not oxidized in aerobic aqueous solution.[23] To examine whether the diacylhydrazine H_2IPH could be responsible for the biological ef-

[a] Department of Chemistry, University of Queensland, Brisbane, Queensland 4072, Australia
Fax: (internat.) + 61-7/3365-4299
E-mail: P.Bernhardt@mailbox.uq.edu.au
[b] Children's Cancer Institute Australia for Medical Research, P. O. Box 81, High St, Randwick, Sydney, New South Wales 2031, Australia

fects of PCIH, their Fe chelation efficacy was compared. Unlike its parent hydrazone, the diacylhydrazine showed little Fe chelation activity, probably because the latter ligand was charged at physiological pH (pH = 7.4), hindering its access across membranes to cellular Fe pools.[23] In contrast, the IPH-Fe complex was charge-neutral, which would permit passage through cell membranes. These data allow a model of Fe chelation for this compound to be proposed: the parent aroylhydrazone (HPCIH) diffuses through cell membranes to bind Fe and is subsequently oxidized to the IPH-Fe complex, which then diffuses from the cell.[23] However, other diacylhydrazine ligands showed much higher activity, probably because they had a neutral charge.[23]

As part of our continuing research into the properties of this class of ligand we have investigated their coordination chemistry with divalent metal ions of the first transition series (Mn to Zn). This was relevant to our work as many of these metal ions are biologically important. From this class of chelators, HPCIH itself was examined as it represented the parent compound of these potential drugs and our earlier studies demonstrated that it possessed interesting properties.[23] For comparison, another member of this group has been assessed in parallel, namely, 2-pyridinecarbaldehyde (4-aminobenzoyl)hydrazone (HPCAH, Scheme 1), which does not bear a potentially bridging N-donor atom. The role of this latter ligating atom in HPCIH was important to assess as it could play a role in the chelation of some transition metal ions and result in different complexes to those found for HPCAH.

We were also interested to assess whether the unprecedented Fe-catalysed oxidation of HPCIH to its diacylhydrazine analogue H_2IPH discovered in our previous investigation[23] could be observed in HPCAH, or in the presence of other metal ions. The results obtained in this study are important for understanding the biological activity of HPCIH and its analogues, especially in terms of their affinity towards other biologically important divalent metal ions that can act as competitors against Fe in vivo.

Results and Discussion

Synthesis and Spectroscopic Properties

Upon reaction of 1 equiv. of the divalent metal ion (chloride salt), 2.5 equiv. of the ligand, and 2 equiv. of Et_3N in methanol, divalent complexes of the general formula ML_2 (M = Mn, Ni, Cu and Zn; L = $PCIH^-$ and $PCAH^-$) were obtained. The 2 equiv. of Et_3N accept protons released from the amide functional group upon complexation. The use of a suitable base was found to be important to afford good yields of the bis(complex), as the same experiments conducted without base gave poor yields or no product at all.

If the same synthesis is applied to the Fe^{II} and Co^{II} analogues, mixtures of products were obtained comprising varying ratios of metal and ligand. The synthesis in MeCN was straightforward by comparison. The Fe^{II} and Co^{II} complexes yield solid-state spin-only magnetic moments of 4.87 and 4.59 B.M., respectively, which are both indicative of high-spin d^6 and d^7 electronic ground states in pseudo-octahedral coordination environments.

In addition to the formation of ML_2 complexes, HPCIH exhibited a variety of other metal/ligand stoichiometries. Complexes of (H)PCIH with metal/ligand ratios of 1:1, 2:2 and 3:2 were obtained, although not with the HPCAH analogue, despite the application of similar conditions. This behaviour may be attributed to the presence of the unhindered N-donor on the isonicotinoyl ring of HPCIH. As seen from crystal structures of the three unusual complexes to be discussed later, the participation of the isonicotinoyl nitrogen atom in coordination evidently changes the way the complexes are formed. By contrast, the free amino group on HPCAH is an ineffective ligand as a result of conjugation of the N-atom lone pair with the aromatic ring.

The free ligand amide N−H (ca. 3450 cm^{-1}) and C=O (ca. 1650 cm^{-1}) stretching vibrations[24,25] are not observed in the IR spectra of the divalent $[M(PCAH)_2]$ and $[M(PCIH)_2]$ complexes. However, the complexes exhibit a strong absorption band at ca. 1600 cm^{-1} not observed in the free ligands, which is due to the conjugated C=N−N=C−O^- moiety.[26] Thus, in each ML_2 complex, the deprotonated ligands are predominantly in the enolate resonance form (Figure 1). The trivalent complex $[Co(PCAH)_2]Cl$ exhibits an IR spectrum essentially the same as the divalent bis complexes. By contrast, the IR spectrum of $[Zn(HPCIH)]SO_4$, where the amide N-atom is not deprotonated, exhibits both the amide N−H and C=O vibration bands (3422, 1684 and 1653 cm^{-1}) and the 1600 cm^{-1} peak characteristic of the deprotonated ligand is absent.

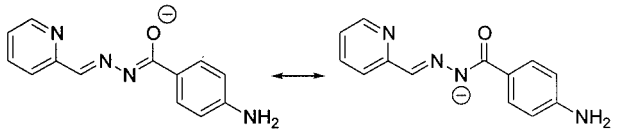

Figure 1. Line drawing of enol and keto resonance forms of $PCAH^-$

The ^{1}H NMR spectrum of $[Co(PCAH)_2]Cl$ shows that both ligands are deprotonated, with the amide-H being absent from the spectrum. In the ^{13}C NMR spectrum, the signals of the carbonyl and imine carbon atoms are shifted downfield by ca. 20 ppm, as expected when this ligand is coordinated through the imine-N and amide-O. Similar results were obtained with the $[Co(PCIH)_2]^+$ analogue.

The electronic spectra of the ML_2 complexes of $PCIH^-$ and $PCAH^-$ in methanol are very similar, and are dominated by intense ligand-based transitions in the near UV region (Table 1). However, the Ni^{II} complexes display weak maxima at ca. 840 nm while complexes of Cu^{II} exhibit maxima at ca. 690 nm, which are both due to d-d transitions. All bis(complexes) show one intense band at ca. 360 nm and one or two less-intense absorptions in the range 240−300 nm. In general, the ligand-based transitions for the (H)PCAH complexes are at lower energy than those for (H)PCIH complexes. Similar red-shifted maxima have been

Table 1. Electronic spectroscopic data (methanol, 298 K)

	λ_{max} [nm] (ε [dm^3 mol^{-1} cm^{-1}])
[Mn(PCAH)$_2$]	389 (24700), 328 (36100)
[Fe(PCAH)$_2$]	633 (2180), 381 (33500), 332 (32800)
[Co(PCAH)$_2$]	392 (25500), 291 (12400)
[Co(PCAH)$_2$]Cl	427 (43900), 284 (26500)
[Ni(PCAH)$_2$]	851 (49), 395 (55000), 295 (19000)
[Cu(PCAH)$_2$]	690 (250), 396 (100000), 300 (47600), 270 (47900)
[Zn(PCAH)$_2$]	391 (35800), 299 (14700), 268 (11600)
[Mn(PCIH)$_2$]	363 (56900), 280 (32400)
[Fe(PCIH)$_2$]	649 (4010), 349 (39000), 268 (19500), 229 (35200)
[Co(PCIH)$_2$]	490 sh (ca. 1000), 356 (30200), 275 (15100)
[Co(PCIH)$_2$]NO$_3$	430 sh (ca. 7700), 381 (17600), 273 (30700)
[Ni(PCIH)$_2$]	857 (21), 373 (17200), 278 (10000)
[Cu(PCIH)$_2$]	699 (53), 367 (25500), 241 (21700)
[Zn(PCIH)$_2$]	363 (25100), 277 (12000)

observed for similar Mn, Fe and Cu complexes when the substituent on the ligand becomes more strongly electron-donating.[27−33] In the electronic spectrum of [Co(PCAH)$_2$]Cl, the intense absorption at ca. 360 nm observed in the other bis(complexes) is shifted significantly to a lower energy at 427 nm (Table 1). This suggests that this electronic transition is of ligand-to-metal charge-transfer origin, with the lower energy reflecting the greater ease of reduction of the trivalent metal ion than the other divalent analogues.

Description of Crystal Structures

HPCAH

The crystal structure of HPCAH·H$_2$O (Table 2) has been determined and a view of the molecule is shown in Figure 2. The bond lengths and angles (Table 3) are as expected for a compound of this type and agree with the other ligands belonging to the HPCIH series.[21] Of note is the C7−O1 bond length, which is typical of a double bond, and the N2−N3 bond, which has a bond order intermediate between a single and a double bond.

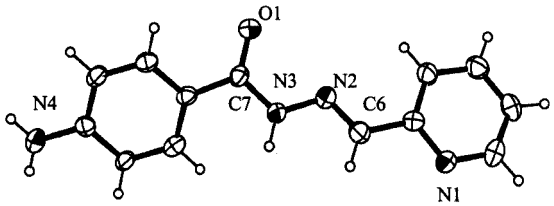

Figure 2. View of HPCAH structure (30% probability ellipsoids)

[M(PCAH)$_2$]·H$_2$O (M = Mn, Ni, Cu and Zn)

The molecular structure of Mn(PCAH)$_2$ is shown in Figure 3. Structures of the Ni^{II}, Cu^{II} and Zn^{II} analogues are very similar and are not shown. Selected bond lengths and angles are listed in Table 3. Each metal ion has a *cis*-N$_4$O$_2$ coordination sphere, where the two deprotonated ligands bind meridionally through their pyridine-N, imine-N and carbonyl-O atoms. The coordinated ligands from two five-membered chelate rings, imposing large distortions on the ideally octahedral coordination angles. The *trans*-N2A−M−N2B angles are close to 180°, whereas the *trans*-N1A(B)−M−O1A(B) angles defined by each meridionally coordinated ligand deviate markedly from linearity; this distortion is greatest for the largest metal ions in the series (Mn^{II} and Zn^{II}). Distortion of the *cis* coordination angles defined by the five-membered chelate rings also increases with metal ion size. The M−N(pyridine), M−N(imine) and M−O bond lengths observed here are within the range reported for other similar complexes of divalent metal ions.[32−36] The variations in C−C, C−N, C−O and N−N bond lengths and angles across the [M(PCAH)$_2$] series are very small, as expected. In general, the average M−N2A(B) distances are significantly shorter than the M−N1A(B) distances, which can be attributed to greater π-back-bonding in the M−N(imine) bond than in the M−N(pyridine)

Table 2. Crystal data for HPCAH and its complexes

	HPCAH·H$_2$O	[Mn(PCAH)$_2$]·H$_2$O	[Ni(PCAH)$_2$]·H$_2$O	[Cu(PCAH)$_2$]·H$_2$O	[Zn(PCAH)$_2$]·H$_2$O
Empirical formula	$C_{13}H_{14}N_4O_2$	$C_{26}H_{24}MnN_8O_3$	$C_{26}H_{24}N_8NiO_3$	$C_{26}H_{24}CuN_8O_3$	$C_{26}H_{24}N_8O_3Zn$
Formula mass	258.28	551.47	555.24	560.07	561.90
Crystal system	orthorhombic	monoclinic	monoclinic	monoclinic	monoclinic
a [Å]	6.38280(5)	9.339(1)	9.379(3)	9.375(2)	9.366(2)
b [Å])	18.2310(2)	13.534(2)	13.616(2)	13.739(1)	13.643(2)
c [Å]	22.071(1)	20.846(3)	20.180(2)	20.147(2)	20.417(3)
β [°]		102.880(3)	103.255(9)	103.330(10)	103.190(10)
V [Å^3]	2568.3(1)	2568.5(6)	2508.4	2525.1	2540.1(8)
T [K]	296	296	296	296	296
Z	8	4	4	4	4
Space group	*Pbca*	*P*2$_1$/*n*	*P*2$_1$/*c*	*P*2$_1$/*n*	*P*2$_1$/*c*
μ (Mo-K_α [mm^{-1}])	0.094	0.559	0.819	0.911	1.012
Indep. reflections (R_{int})	2253 (0.000)	4510 (0.0347)	4400 (0.0732)	4431 (0.0724)	4464 (0.0767)
R_1 (obsd. data)	0.0490	0.0657	0.0695	0.0524	0.0703
wR_2	0.1139	0.1650	0.1274	0.1163	0.1445

Table 3. Selected bond lengths [Å] and angles [°] of free ligand and metal complexes of HPCAH

	$HPCAH·H_2O$	$[Mn(PCAH)_2]·H_2O$	$[Ni(PCAH)_2]·H_2O$	$[Cu(PCAH)_2]·H_2O$	$[Zn(PCAH)_2]·H_2O$
M−N1A	−	2.321(5)	2.095(7)	2.180(6)	2.259(7)
M−N1B	−	2.282(5)	2.125(7)	2.234(7)	2.207(7)
M−N2A	−	2.170(4)	1.976(7)	1.949(6)	2.048(7)
M−N2B	−	2.169(4)	1.976(7)	1.956(6)	2.051(7)
M−O1A	−	2.137(4)	2.100(6)	2.124(5)	2.113(6)
M−O1B	−	2.152(4)	2.100(6)	2.173(5)	2.139(5)
N1A−M−O1A	−	143.76(15)	154.8(3)	154.6(2)	150.4(2)
N1B−M−O1B	−	142.95(16)	155.2(3)	152.6(2)	149.9(2)
N2A−M−N2B	−	173.72(17)	178.7(4)	178.0(3)	175.2(3)
N1A−M−N1B	−	90.45(17)	93.9(3)	93.0(2)	91.7(2)
N1A−M−N2B	−	102.05(16)	102.3(3)	101.5(2)	100.0(3)
N2A−M−N1B	−	106.32(17)	100.2(3)	104.7(2)	105.1(2)
N1A−M−N2A	−	71.82(17)	78.5(3)	77.8(2)	75.3(3)
N2A−M−O1A	−	72.20(15)	76.4(3)	76.8(2)	75.2(3)
C6A−N2A	1.265(7)	1.290(7)	1.260(11)	1.282(9)	1.261(10)
C6B−N2B	−	1.256(7)	1.274(11)	1.281(9)	1.259(10)
C7A−N3A	1.374(8)	1.362(7)	1.350(11)	1.344(9)	1.347(10)
C7B−N3B	−	1.324(7)	1.349(10)	1.344(10)	1.338(10)
C7A−O1A	1.228(7)	1.276(6)	1.268(9)	1.274(8)	1.267(8)
C7B−O1B	−	1.280(6)	1.257(9)	1.256(8)	1.272(9)
N2A−N3A	1.365(6)	1.365(6)	1.367(9)	1.360(7)	1.367(9)
N2B−N3B	−	1.372(6)	1.361(9)	1.380(7)	1.369(8)

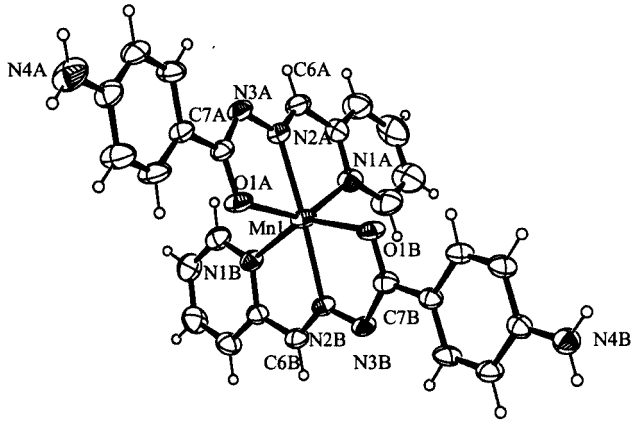

Figure 3. View of the $[Mn(PCAH)_2]$ molecule (30% probability ellipsoids)

bond[36,37] and also to the steric requirements of the meridionally coordinated ligand.

Although the C6A(B)−N2A(B) and N2A(B)−N3A(B) bond lengths are unaffected by complexation [ca. 1.27 and 1.37 Å in the complexes compared with 1.265(7) and 1.365(6) Å in the free ligand, respectively], the C7A(B)−O1A(B) bond lengthens significantly (by ca. 0.04 Å); variations in the C7A(B)−N3A(B) bond upon complexation are less pronounced. Overall, these observations are consistent with the enolate resonance form of the ligand (Figure 1) being dominant in the deprotonated coordinated ligand, and this is supported by the IR spectroscopic data.[36,38−45]

HPCIH Complexes

Crystal data and selected bond lengths and angles of the various HPCIH complexes are given in Tables 4 and 5 respectively. The molecular structure of $[Cu(PCIH)_2]$ is shown in Figure 4. The four (Cu, Ni and both Co) bis(complexes) of HPCIH share common structural characteristics with the ML_2 complexes of $PCAH^-$ described above. All metal ions have *cis*-N_4O_2 coordination spheres, where each of the two ligands binds the metal ion meridionally via the pyridine-N, imine-N and carbonyl-O atoms. In most cases the bond lengths in the $[M(PCIH)_2]$ complexes (Table 5) are similar to those found in $PCAH^-$ analogues (Table 3). This implies that the coordinated HPCIH ligand also exists predominantly in the enolate resonance form with the conjugated C=N−N=C−O^- moiety, agreeing with the IR spectra.

Two Co^{III} complexes of HPCIH were isolated, shown in Figures 5 and 6. $[Co(HPCIH)(PCIH)](NO_3)_2$ exhibits a structure (Figure 5) similar to the Cu^{II} and Ni^{II} bis(complexes), except that one of the ligands is protonated at its isonicotinoyl N-atom; i.e., the protonated ligand is present in a zwitterionic (pyridinium/amidate) form. The other cobalt complex of HPCIH consists of two cobalt ions: an octahedral Co^{III} coordinated within the expected N_4O_2 donor set and a tetrahedral Co^{II} ion coordinated to three chloride ions and the nitrogen atom of the isonicotinoyl ring (Figure 6, Table 6). Since a 1:2 ratio of Co/HPCIH was used in the synthesis, the formation of this complex may be attributed to the strong tendency for the free isonicotinoyl nitrogen atom to coordinate.

The fact that DMSO is an effective ligand, together with the presence of residual chloride ions and the strongly coordinating isonicotinoyl nitrogen atom, are compounding reasons that lead to the isolation of $[\{MnCl_2(DMSO)(HPCIH)\}_2Mn(DMSO)_2Cl_2]$, as an unusual M_3L_2 complex (Figure 7, Table 6). The bridging Mn (Mn1), at a centre of symmetry, bears no chelate rings, so all *cis* coordination angles are close to 90°. The coordination

Table 4. Crystal data of metal complexes of HPCIH

	[{$MnCl_2$(DMSO)-(HPCIH)}$_2$Mn(DMSO)$_2Cl_2$]	[Co(PCIH)$_2CoCl_3$]·$2H_2O$	[Co(HPCIH)(PCIH)]-$(NO_3)_2$·H_2O·$^1/_2CH_3OH$	[Ni(PCIH)$_2$]·$2H_2O$	[Cu(PCIH)$_2$]	[Zn(HPCIH)]SO_4·$3^1/_2H_2O$
Empirical formula	$C_{32}H_{44}Cl_6Mn_3N_8O_6S_4$	$C_{24}H_{22}Cl_3Co_2N_8O_4$	$C_{24.5}H_{23}CoN_{10}O_{9.5}$	$C_{24}H_{22}N_8NiO_4$	$C_{24}H_{18}CuN_8O_2$	$C_{12}H_{17}N_4O_{8.5}SZn$
Formula mass	1142.52	710.71	688.46	545.21	514.00	450.73
Crystal system	monoclinic	triclinic	triclinic	triclinic	monoclinic	monoclinic
a [Å]	17.169(4)	12.101(1)	9.947(1)	8.2500(9)	8.2361(5)	6.654(2)
b [Å]	7.1321(5)	12.3805(9)	12.741(2)	8.656(2)	20.290(3)	15.034(2)
c [Å]	20.389(3)	13.542(2)	13.744(2)	17.305(3)	13.695(1)	16.878(4)
α [°]		97.726(8)	62.27(1)	91.17(2)		
β [°]	105.82(2)	116.009(9)	72.472(9)	94.86(1)	102.518(7)	97.90(3)
γ [°]		107.599(7)	84.753(9)	93.03(1)		
V [Å^3]	2402.1(7)	1651.4(3)	1467.8(3)	1229.2(4)	2234.2(4)	1672.4(7)
T [K]	296	296	296	296	296	296
Z	4	2	2	2	4	4
Space group	$P2_1/a$	$P\bar{1}$	$P\bar{1}$	$P\bar{1}$	$P2_1/a$	$P2_1/n$
μ [mm^{-1}]	1.332	1.287	0.656	0.837	1.019	1.649
Indep. reflections (R_{int})	4232 (0.0286)	5785 (0.0878)	5144 (0.0243)	4323 (0.0496)	3908 (0.0367)	2930 (0.0392)
R_1 (obsd. data)	0.0841	0.1018	0.0715	0.0554	0.0408	0.0459
wR_2	0.2110	0.2788	0.2242	0.1204	0.0942	0.1019

Table 5. Selected bond lengths [Å] and angles [°] for mononuclear metal complexes of HPCIH

	[Co(HPCIH)(PCIH)]$(NO_3)_2$·H_2O·$^1/_2CH_3OH$	[Ni(PCIH)$_2$]·$2H_2O$	[Cu(PCIH)$_2$]	[Zn(HPCIH)]SO_4·$3^1/_2H_2O$
M−N1A	1.920(5)	2.109(5)	2.118(3)	2.120(5)
M−N1B	1.915(4)	2.128(4)	2.301(4)	–
M−N2A	1.848(5)	1.975(4)	1.946(3)	2.091(5)
M−N2B	1.858(5)	1.976(4)	1.992(3)	–
M−O1A	1.915(4)	2.121(4)	2.096(3)	2.219(4)
M−O1B	1.918(4)	2.093(4)	2.328(3)	–
N1A−M−O1A	165.11(18)	154.48(15)	153.36(12)	149.25(17)
N1B−M−O1B	165.02(18)	153.63(16)	148.58(11)	–
N2A−M−N2B	176.6(2)	176.7(2)	172.00(15)	–
N1A−M−N1B	92.0(2)	87.17(18)	97.20(13)	–
N1A−M−N2B	99.7(2)	103.67(18)	104.45(13)	–
N2A−M−N1B	99.3(3)	99.40(18)	96.03(13)	–
N1A−M−N2A	83.0(2)	78.62(19)	78.12(13)	76.62(18)
N2A−M−O1A	82.12(19)	75.87(17)	77.04(12)	72.71(15)
C6A−N2A	1.278(8)	1.288(7)	1.284(5)	1.254(7)
C6B−N2B	1.286(7)	1.282(7)	1.277(5)	–
C7A−N3A	1.309(8)	1.334(7)	1.333(5)	1.345(7)
C7B−N3B	1.322(7)	1.339(7)	1.332(5)	–
C7A−O1A	1.299(7)	1.255(6)	1.269(4)	1.230(7)
C7B−O1B	1.289(7)	1.267(6)	1.250(5)	–
N2A−N3A	1.381(7)	1.382(6)	1.360(4)	1.359(6)
N2B−N3B	1.375(6)	1.358(6)	1.367(5)	–

sphere comprises two DMSO ligands, two chloride ions and two isonicotinoyl residues. The symmetry-related Mn ions (Mn2 and Mn2′) are each coordinated in a tridentate fashion to an HPCIH ligand. It is interesting to note that the two chloride ions on the central Mn1 are *trans* oriented, whereas on Mn2 the chloride ions are *cis*. A large distortion from octahedral geometry is imposed by the tridentate coordinated HPCIH ligand on the ideally linear N1−Mn−O1 bond angle, which is contracted to 138.1(2)°. No substantial C7−O1 bond lengthening or C7−N3 bond shortening is observed in the complex relative to free ligand. The amide N3 atom is not deprotonated, thus preventing the formation of enolate ion and the conjugated C=N−N=C−O$^-$ moiety.

In the case of [Zn(HPCIH)SO_4], the participation of the isonicotinoyl nitrogen atom and sulfate anions in coordination led to a surprising result (Figure 8). The N_2O-tridentate HPCIH is again bonded to Zn^{II} meridionally in addition to an isonicotinoyl nitrogen atom *trans* to the imine nitrogen atom. These ZnN_3O moieties are arranged in parallel planes, with bridging sulfate anions occupying the sites perpendicular to this plane. The result is a three-dimensional coordination polymer. This mode of coordination is in contrast to the other complexes reported herein, which

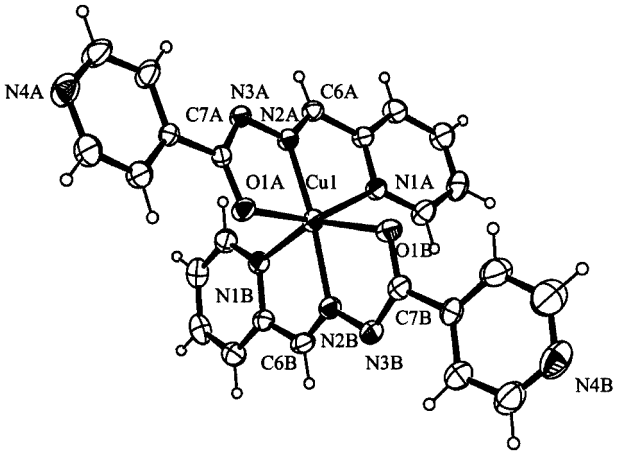

Figure 4. View of the $[Cu(PCIH)_2]$ molecule (30% probability ellipsoids)

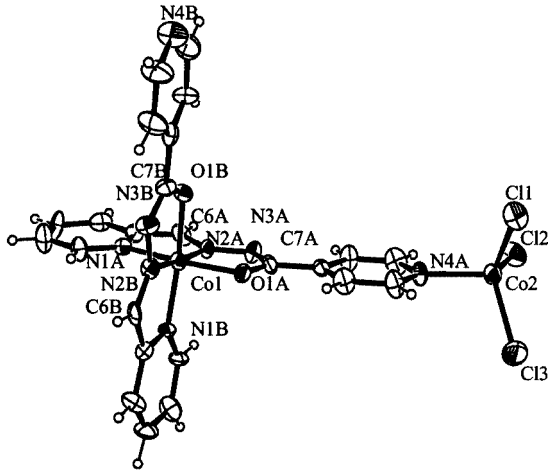

Figure 6. View of the $[Co(PCIH)_2CoCl_3]$ molecule (30% probability ellipsoids)

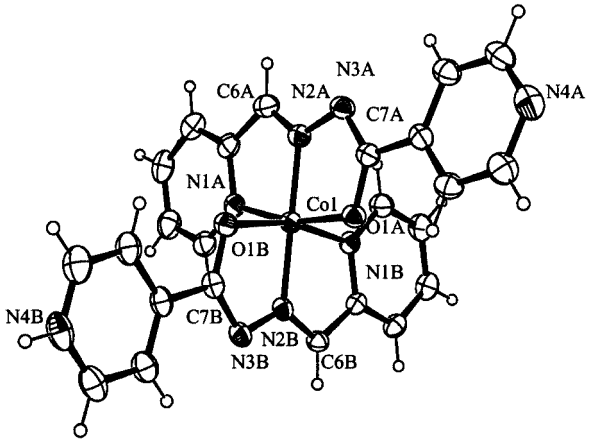

Figure 5. View of the $[Co(HPCIH)(PCIH)]^{2+}$ cation (30% probability ellipsoids)

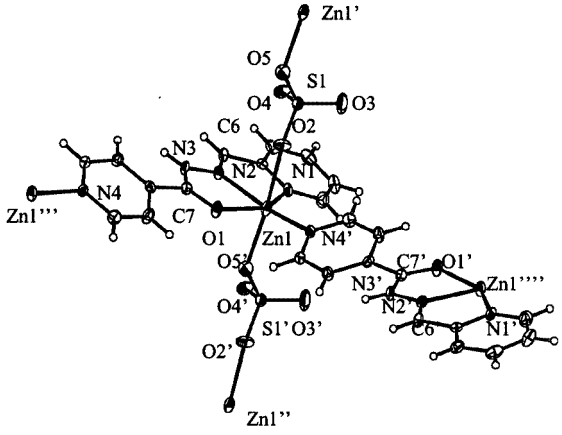

Figure 8. Partial view of the polymeric $[Zn(HPCIH)]SO_4$ structure (30% probability ellipsoids)

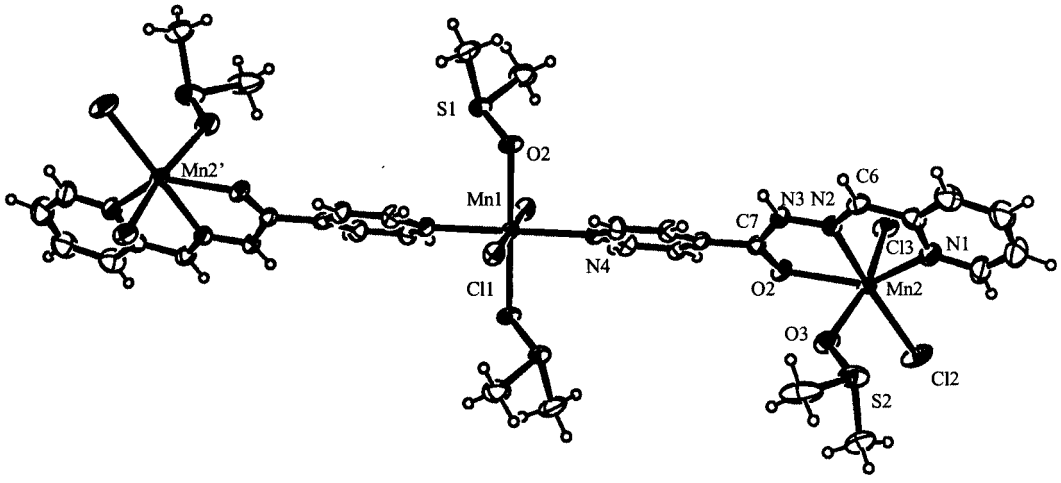

Figure 7. View of $[\{MnCl_2(DMSO)(HPCIH)\}_2Mn(DMSO)_2Cl_2]$ structure (30% probability ellipsoids)

are discrete molecules. While the *trans*-O2−Zn−O3′ and -N2−Zn−N4′ bonds are almost linear, the *trans*-N1−Zn−O1 bond is bent to 149.3(2)°. The C7−O1 and C7−N3 bond lengths in this complex are similar to those in the free ligand. The fact that the hydrazone remains protonated in this complex results in these bonds retaining their double bond character in the absence of the electron delocalisation seen in the complexed deprotonated ligands.

Table 6. Selected bond lengths [Å] and angles [°] of oligonuclear HPCIH complexes

	[{$MnCl_2$(DMSO)-(HPCIH)}$_2$Mn(DMSO)$_2Cl_2$]	[Co(PCIH)$_2$-$CoCl_3$]·$2H_2O$
M1−N1A	2.312(6)	1.925(13)
M1−N1B	−	1.896(13)
M1−N2A	2.258(6)	1.850(12)
M1−N2B	−	1.847(13)
M1−O1A	2.311(4)	1.907(11)
M1−O1B	−	1.915(11)
M2−N4A	2.292(5)	2.034(13)
M2−Cl3	2.499(2)	2.242(7)
N1A−M1−O1A	138.14(19)	165.1(5)
N1B−M1−O1B	−	165.4(5)
N2A−M1−N2B	−	174.4(7)
N1A−M1−N1B	−	91.7(6)
N1A−M1−N2B	−	99.2(6)
N2A−M1−N1B	−	101.4(6)
N1A−M1−N2A	69.2(2)	82.7(6)
N2A−M1−O1A	68.96(17)	82.4(5)
N4A−M2−Cl3	88.14(14)	105.6(5)
C6A−N2A	1.266(8)	1.27(2)
C6B−N2B	−	1.29(2)
C7A−N3A	1.344(8)	1.32(2)
C7B−N3B	−	1.31(2)
C7A−O1A	1.233(8)	1.326(19)
C7B−O1B	−	1.309(19)
N2A−N3A	1.356(7)	1.348(17)
N2B−N3B	−	1.375(19)

Overall, it can be concluded that the active participation of the isonicotinoyl nitrogen of HPCIH in bonding has led to a much more varied and unpredictable coordination chemistry.

EPR Spectroscopy of Copper(II) Complexes

The Jahn−Teller distortions observed in most six-coordinate Cu^{II} complexes[46] are revealed in the crystal structure of [Cu(PCIH)$_2$], where the *trans*-Cu−N1B and -Cu−O1B bonds are exceptionally long [2.301(4) and 2.328(3) Å, respectively] compared to the other four coordination bonds (Table 5). However, this distortion is not apparent in the structure of [Cu(PCAH)$_2$]·H_2O (Table 3). EPR spectroscopy was employed to resolve this issue. [Cu(PCIH)$_2$] and [Cu(PCAH)$_2$] exhibit identical EPR spectra (Figure 9) and these could be simulated with identical, axially symmetric spin Hamiltonian parameters ($g_{\|}$ = 2.262, $g_{\perp}$ = 2.09, $A_{\|}$ = 122 *G* and $A_{\perp}$ = 25 G). These parameters are consistent with a tetragonally elongated d^9 complex in a $d_{x^2-y^2}$ ground state ($g_{\|} > g_{\perp}$ and $A_{\|} > A_{\perp}$) with significant distortion of the in-plane *cis* coordinate angles away from 90° ($A_{\|} <<$ 200 G). Note that the broad feature around 3300 G ($g \approx$ 2) is due to an impurity in the EPR spectrometer cavity, and so the experimental and simulated spectra are obviously different in this region. The EPR results indicate that the copper ions are in the same electronic environment in both [Cu(PCIH)$_2$] and [Cu(PCAH)$_2$] despite their apparent structural differences. That is, the bond lengths found in [Cu(PCIH)$_2$] are representative of the true tetragonally elongated structures of both [Cu(PCIH)$_2$] and [Cu(PCAH)$_2$], whereas the geometry defined by the crystal structure of [Cu(PCAH)$_2$] is a weighted average of two tetragonally elongated forms, and thus apparently (but not really) tetragonally compressed.

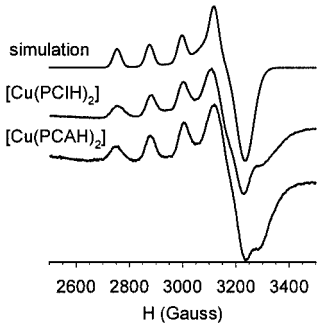

Figure 9. Experimental X-band (9.303 GHz) EPR spectra of [Cu(PCAH)$_2$] (bottom) and [Cu(PCIH)$_2$] (centre): conditions: 1 mM complex in DMF/H_2O (1:2), 77 K; the simulated spectrum is shown at the top (see text for simulation parameters); broad, high-field resonances ($g \approx 2$) in experimental spectra are due to cavity impurities

Ligand Oxidation

One interesting observation while preparing the Co-HPCIH complexes was that the HPCIH ligand is not oxidised when the redox-active Co^{II} is oxidised to Co^{III} by dissolved atmospheric oxygen in the solution during complex formation. This is in contrast to our earlier report of the oxidation of HPCIH to the diacylhydrazine *N*-(isonicotinoyl)-*N*′-(picolinoyl)hydrazone (H_2IPH) while trying to prepare the Fe^{III} complex of HPCIH.[23] We successfully duplicated the preparation of the trivalent complex [Fe(HIPH)(IPH)] from Fe^{II} salts and HPCIH as starting materials, but as yet have been unable to isolate the trivalent [Fe(PCIH)$_2$]$^+$ complex. We believe that the ligand oxidation is not a straightforward process. Indeed, it probably involves Fe^{III}, water and O_2 in the mechanism, since a similar oxidation is not observed with Co^{II} and Co^{III}, or any other transition metals investigated in this report. Nevertheless, the divalent [FeL_2] (L = PCIH and PCAH) complexes have been synthesised and the [Fe(PCIH)$_2$] complex formation constants have been demonstrated by potentiometric titration (see below). So far our work on HPCAH has not shown any evidence of ligand oxidation in the presence of either Fe^{II} or Fe^{III}. This adds another dimension to the ligand oxidation phenomenon such that oxidation seems to be peculiar to HPCIH. We are currently working toward an understanding of this oxidation mechanism.

Formation Constants

The formation constants of the bis(complexes) of HPCIH with divalent first-row transition metals from manganese to zinc have been determined. The results are shown in Table 7. The values obtained are similar to those obtained with similar tridentate ligands and consistent with the Irving−Williams order.[47] The exceptionally low log K_2 value ($ML + L \rightleftarrows ML_2$) of Cu^{II} at 7.42 is expected, since

the addition of a second ligand forces the Cu^{II} centre into a strained tetragonally elongated six-coordinate configuration evident from the crystal structure (Table 5) and EPR spectrum (Figure 9) of $[Cu(PCIH)_2]$, where the rigid meridionally coordinated second ligand must span the elongated axis of the coordination sphere.

Table 7. Formation constants of complexes of (H)PCIH with divalent first row transition metals

	Mn^{II}	Fe^{II}	Co^{II}	Ni^{II}	Cu^{II}	Zn^{II}
$\log K_1$ (ML)	4.71(3)	7.02(3)	7.67(5)	9.27(4)	10.83(8)	7.41(7)
$\log\beta_2$ (ML_2)	9.20(3)	13.37(2)	14.42(5)	16.97(4)	18.25(9)	13.85(7)

A typical speciation plot, such as that for the Ni^{II} complex shown in Figure 10, illustrates the transition from free metal ions to bis(complexes) as pH increases. At lower pH, the monoligand complex is the prevailing species, with $[Ni(PCIH)]^+$ beginning to form at pH = 2.5 (while $[Cu(PCIH)]^+$ begins to form at pH = 1.5). As the pH increases, bis(complexes) begin to form, eventually becoming the only species at pH = 7 and beyond. The Mn^{II} complex is the exception due to the closeness of log K_1 ($M + L \rightleftarrows ML$) and log K_2 ($ML + L \rightleftarrows ML_2$) values (4.71 and 4.49, respectively). $[Mn(PCIH)]^+$ only begins to form at pH = 5 while $[Mn(PCIH)_2]$ begins to form at pH = 7. Both species coexist in equilibrium through to pH = 12. Thus, the isolation of $[\{MnCl_2(DMSO)(HPCIH)\}_2Mn(DMSO)_2Cl_2]$ can be further rationalised by considering the formation constants, which illustrate that the formation of $[Mn(PCIH)_2]$ is least favourable of all ML_2 metal complexes in this series.

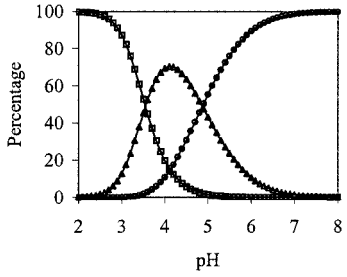

Figure 10. pH speciation plot for Ni^{II} complexes of HPCIH; key: squares: free Ni^{2+} ions; triangles: $[Ni(PCIH)]^+$; circles: $[Ni(PCIH)_2]$

Biological Activity

The Fe chelation efficacy of the HPCIH analogues is now established.[19−21] An important question concerns the physiologically relevant form of these chelators and their complexes upon encountering intracellular Fe and other competing metal ions. The HPCIH analogues form divalent Fe complexes even in the presence of oxygen. This is in contrast with other biologically active Fe chelators such as DFO, which spontaneously oxidises Fe^{II} to its trivalent state under aerobic conditions.

Given the reactivity of the Fe^{III} complex of $PCIH^-$ and the ready formation of the divalent complex in our synthetic studies,[23] it appears that the trivalent complexes of the HPCIH analogues will not be the major species in vivo, and the biological activity of the chelators may be attributed to their ability to act as intracellular Fe^{II} chelators rather than Fe^{III} chelators. The formation constants of HPCIH with Fe^{II} are not particularly high (Table 7) and there is nothing to suggest that the ligands are selective for divalent Fe over any of the other metal ions. In fact, at face value, the ligands should form more stable divalent complexes with Cu and Zn which are also present in biological fluids. However, intracellular Fe is present in much higher concentrations than other transition metals, and this will naturally influence the outcome under physiological conditions.

It is well known that charge neutrality and lipophilicity are desirable features in facilitating passage across cell membranes and thus enhancing Fe mobilisation activity. It is pertinent that the divalent complexes of HPCIH are charge-neutral, so the metal-free chelators may enter the cell in a charge-neutral form and the Fe complexes also may leave the cell in a charge-neutral form. A similar charge neutrality has been sought in tribasic ligands such as DFO and tris-L1 in complexes with trivalent Fe. Although the FeL_2 (L = PCIH, PCAH) complexes may be oxidised to their trivalent forms with mild oxidants, they are highly reactive and would be unlikely to survive in vivo. Furthermore, they would necessarily carry a positive charge, which may inhibit their exit from the cell.

An alternative, but less likely, hypothesis to explain the pronounced Fe mobilisation activity of these chelators is that ligand dehydrogenation of the unstable trivalent Fe complexes of the HPCIH (hydrazone) analogues occurs generating the corresponding hydrazine (H_2IPH) complex within the cell, by analogy with observations of the chemistry of these complexes on a preparative scale.[23] At this point, we prefer the former argument, as the hydrazine analogue of HPCIH (H_2IPH) exhibits very poor Fe mobilisation activity,[23] and its biological role in the activity of the HPCIH analogues is doubtful. Even though the formation constants of bis(complexes) of HPCAH with divalent first-row transition metals have not been determined, we would expect their values to exhibit the same trend and order of magnitude as those of HPCIH due to the similarities of the two ligands. In fact, the crystallographic and spectroscopic data reported herein show that the local coordination environments of the $[M(PCIH)_2]$ and $[M(PCAH)_2]$ complexes are indistinguishable. The main feature that distinguishes the HPCIH analogues in terms of their biological activity appears to be their lipophilicity, which affects their ability to cross the cell membrane and gain access to intracellular Fe pools.

Conclusion

Divalent first-row transition metals (Mn, Fe, Co, Ni, Cu and Zn) readily form similar bis(complexes) with HPCAH as shown by spectroscopy and X-ray crystallography. How-

ever, complexes of HPCIH are less predictable, forming complexes of various metal/ligand ratios. Such behaviour is attributed to the active participation of the unhindered isonicotinoyl nitrogen atom in bonding. In the case of the trinuclear complex $[\{MnCl_2(DMSO)(HPCIH)\}_2Mn(DMSO)_2Cl_2]$, the low formation constant of $[Mn(PCIH)_2]$ coupled with competition from ligands like DMSO and chloride, as well as participation of the isonicotinoyl nitrogen atom in coordinate bonding, led to the formation of this unique compound. From the IR spectra and crystal data, it is evident that the deprotonated hydrazone ligands exist predominantly in the enolate resonance form. Oxidation of HPCIH and HPCAH in the presence of divalent metal ions was not observed in this study, which further strengthens our belief that the unique participation of Fe^{III} and oxygen is the key to this unprecedented oxidation of HPCIH to H_2IPH. On the other hand, formation constants of the divalent metal complexes of HPCIH show that the affinity of this ligand for Fe^{II} is not particularly great, although the chelator is successful in mobilising iron as shown by our cell culture experiments.[23] Other factors such as the greater bioavailability of Fe or, less likely, the intracellular oxidation of HPCIH to H_2IPH could be the answer and further studies are being undertaken to ascertain these unresolved questions.

Experimental Section

Materials: The chemicals and solvents used in this work were of analytical grade, available commercially, and were used without further purification.

Physical Measurements: Solution UV/Vis spectra were measured with a Perkin−Elmer Lambda 40 spectrophotometer. Infrared spectra were measured with a Perkin−Elmer 1600 series instrument, with compounds being dispersed as KBr discs. ^1H NMR spectra were obtained with a Bruker AC200F spectrometer using TMS as the internal standard. Electron paramagnetic resonance (EPR) spectra were recorded at 77 K with a Bruker ER200D spectrometer at X-band frequency (9.303 GHz). Samples were made up as 1 mM solutions in a DMF/water (1:2) mixture. Spectra were simulated with the program EPR50F.[48] Potentiometric titrations were performed under nitrogen at 298 K with a Metrohm E665 Dosimat autotitrator equipped with a 5-mL burette. The titrant was 0.1 M Et_4NOH standardised with HCl. Solutions of pure ligands (1 mM) were used in the titrations for the determination of protonation constants. The chelators were prepared in $HClO_4$ (6 mM) and Et_4NClO_4 (0.1 M) as supporting electrolyte to maintain a constant ionic strength throughout the titration. Solutions of transition metal ions plus ligands used in the titration for the determination of metal complex formation constants contained transition metal ions as the perchlorate salt (0.5 mM), ligand (1.25 mM) (calculated at a 1:2 metal ion/ligand ratio, with 25% excess ligand added), $HClO_4$ (6−12 mM) and Et_4NClO_4 (0.1 M). Care was taken to pre-purge all solutions with nitrogen so as to prevent complications from redox reactions. Milli-Q water was used to make up the transition metal salt solutions, which were also pre-purged with nitrogen before dissolution. The solution potential was measured using an Orion 720A pH meter and an Ionode IJ44 intermediate junction pH electrode. The electrode was calibrated by strong acid-strong base titration prior to every potentiometric titration of the ligands or complexes. Data obtained were fitted to the Nernst equation and the pK_a values or formation constants were determined using the program SuperQuad.[49] In each case, a minimum of four titrations was performed in the range $2 < pH < 12$.

Ligand Syntheses: HPCIH and HPCAH were synthesised by a Schiff-base condensation between 2-pyridinecarbaldehyde and the respective acid hydrazides as described previously.[20,21,50] Slow concentration of an aqueous methanol (1:1) solution of HPCAH afforded crystals suitable for X-ray work.

HPCIH·2H$_2$O: $C_{12}H_{14}N_4O_3$ (262.2): calcd. C 54.96, H 5.38, N 21.36; found C 55.10, H 5.34, N 21.55. IR: $\tilde{\nu}_{max}$ = 3448 s, 3050 w, 3007 w, 1681 vs, 1660 vs, 1552 vs, 1473 s, 1437 s, 1411 s, 1370 s, 1293 vs, 1147 s, 1071 s, 1002 w, 929 w, 845 w, 783 s, 742 s, 692 vs, 625 w and 521 w cm^{-1}. ^1H NMR ([D$_4$]methanol):δ = 7.47 (m, 1 H), 7.92 (m, 3 H), 8.28 (d, 1 H), 8.45 (s, 1 H), 8.60 (m, 1 H) and 8.78 (dd, 2 H) ppm. ^{13}C NMR ([D$_4$]methanol):δ = 122.4, 123.2, 126.3, 138.7, 142.1, 150.3, 150.7, 151.1, 154.1 and 164.9 ppm.

HPCAH·H$_2$O: $C_{13}H_{14}N_4O_2$ (258.3): calcd. C 60.46, H 5.46, N 21.69; found C 60.43, H 5.42, N 21.65. IR: $\tilde{\nu}_{max}$ = 3528 s, 3466 s, 3434 vs, 3316 s, 3208 s, 3034 w, 2987 w, 1646 vs, 1629 vs, 1603 vs, 1551 s, 1514 s, 1472 s, 1434 s, 1348 s, 1283 vs, 1183 vs, 1150 s, 1076 w, 1000 w, 938 w, 843 s, 770 w, 744 w, 694 s, 666 w and 620 s cm^{-1}. ^1H NMR ([D$_6$]DMSO): δ = 5.87 (s, 1 H), 6.63 (d, 2 H), 7.36 (m, 1 H), 7.72 (d, 2 H), 7.86 (m, 2 H), 8.44 (s, 1 H), 8.58 (d, 1 H) and 11.73 (s, 1 H). ^{13}C NMR ([D$_6$]DMSO): δ = 112.9, 119.4, 119.9, 124.3, 129.9, 137.0, 146.4, 149.7, 152.8, 153.9 and 163.7 ppm.

Complex Syntheses

Bulk Syntheses of [M(PCIH)$_2$] and [M(PCAH)$_2$] Complexes (M = Mn, Ni, Cu and Zn): The ligand (HPCIH or HPCAH; 2.5 mmol) was dissolved in 30 mL of methanol. The chloride salt of the respective metal (1 mmol) was added to the solution, followed by triethylamine (Et_3N; 2 mmol). The mixture was gently refluxed for 3 h and then concentrated to approximately one third of the original volume. The resulting precipitate was collected by vacuum filtration and washed with distilled water. Complexes ML_2 of Mn^{II}, Ni^{II} and Cu^{II} were all brown in colour, while the Zn^{II} complexes were bright yellow. Yields of the first crops of compound were 20−40%. Further crops were obtained from concentration of the filtrates.

Bulk Syntheses of [M(PCIH)$_2$] and [M(PCAH)$_2$] Complexes (M = Fe and Co): The ligand (HPCIH or HPCAH; 4 mmol) was dissolved in 50 mL of MeCN. Triethylamine (30 mmol) was added, followed by the perchlorate salt of the respective metal (1.6 mmol). The mixture was gently refluxed for 3 h and then concentrated to approximately one third of the original volume. The resulting precipitate was collected by vacuum filtration and washed with MeOH and then with distilled water. The Fe^{II} complexes were green and the Co^{II} complexes were deep purple. Yields of the first crops of compound were 75−80%.

[Mn(PCIH)$_2$]·H$_2$O: $C_{24}H_{20}MnN_8O_3$ (524.4): calcd. C 55.07, H 3.85, N 21.41; found C 54.97, H 3.42, N 21.38. IR: $\tilde{\nu}_{max}$ = 3070 w, 3023 w, 1607 s, 1591 s, 1568 s, 1497 vs, 1487 vs, 1460 vs, 1358 vs, 1308 s, 1150 s, 1068 vs, 782 w, 755 s and 699 s cm^{-1}.

[Fe(PCIH)$_2$]·0.5H$_2$O: $C_{24}H_{10}FeN_8O_{2.5}$ (515.3): calcd. C 55.94, H 3.72, N 21.74; found C 55.42, H 3.44, N 21.79. IR: $\tilde{\nu}_{max}$ = 3072 w, 3021 w, 1601 s, 1566 s, 1498 vs, 1482 vs, 1456 vs, 1362 vs, 1344 vs, 1308 s, 1151 s, 1063 vs, 784 w, 754 s and 700 s cm^{-1}.

[Co(PCIH)$_2$]: $C_{24}H_{18}CoN_8O_2$ (509.4): calcd. C 56.59, H 3.56, N 22.00; found C 56.67, H 3.53, N 22.03. IR: $\tilde{\nu}_{max}$ = 3014 w, 1604 s, 1567 s, 1484 vs, 1457 vs, 1359 vs, 1308 s, 1149 s, 1072 vs, 785 w, 755 s and 700 s cm^{-1}.

[Ni(PCIH)$_2$]·3H$_2$O: $C_{24}H_{24}N_8NiO_5$ (563.2): calcd. C 51.18, H 4.30, N 19.90; found C 51.57, H 3.82, N 19.78. IR: $\tilde{\nu}_{max}$ = 1609 vs, 1567 s, 1488 vs, 1460 vs, 1357 vs, 1153 s, 1312 s, 1153 s, 1078 vs, 784 w, 758 s and 701 s cm^{-1}.

[Cu(PCIH)$_2$]: $C_{24}H_{18}CuN_8O_2$ (514.0): calcd. C 56.08, H 3.53, N 21.80; found C 55.84, H 3.51, N 21.61. IR: $\tilde{\nu}_{max}$ = 3068 w, 3020 w, 1603 s, 1586 s, 1570 vs, 1519 vs, 1486 vs, 1458 vs, 1364 vs, 1351 vs, 1339 vs, 1306 vs, 1151 s, 1064 vs, 784 s, 754 s and 700 s cm^{-1}.

[Zn(PCIH)$_2$]·0.5H$_2$O: $C_{24}H_{19}N_8O_{2.5}Zn$ (524.9): calcd. C 54.92, H 3.65, N 21.35; found C 55.22, H 3.45, N 21.63. IR: $\tilde{\nu}_{max}$ = 3072 w, 3020 w, 1609 w, 1591 s, 1569 s, 1500 vs, 1486 vs, 1462 vs, 1355 vs, 1307 s, 1149 s, 1073 s, 784 s, 756 s and 700 s cm^{-1}.

[Mn(PCAH)$_2$]·H$_2$O: $C_{26}H_{24}MnN_8O_3$ (551.4): calcd. C 56.63, H 4.39, N 20.32; found C 56.42, H 4.41, N 19.99. IR $\tilde{\nu}_{max}$ = 3354 s, 3210 s, 2677 w, 1624 s, 1599 vs, 1551 w, 1484 s, 1456 s, 1421 s, 1354 vs, 1291 vs, 1174 vs, 1146 vs, 1102 s, 1070 vs, 914 w, 851 w, 767 s, 678 w, 637 s and 503 w cm^{-1}.

[Fe(PCAH)$_2$]·2.5H$_2$O: $C_{26}H_{27}N_8O_{4.5}Fe$ (579.4): calcd. C 53.90, H 4.70, N 19.34; found C 54.08, H 4.26, N 19.34. IR: $\tilde{\nu}_{max}$ = 3332 s, 3214 s, 1632 s, 1604 vs, 1560 w, 1472 s, 1448 s, 1411 s, 1363 vs, 1289 vs, 1175 vs, 1150 vs, 1110 s, 1068 vs, 846 w, 761 s, 681 w and 506 w cm^{-1}.

[Co(PCAH)$_2$]·H$_2$O: $C_{26}H_{24}$ Co N_8O_3 (555.5): calcd. C 56.22, H 4.35, N 20.17; found C 55.90, H 4.46, N 19.97. IR: $\tilde{\nu}_{max}$ = 3344 s, 3214 s, 1628 s, 1598 vs, 1548 w, 1482 s, 1456 s, 1420 s, 1354 vs, 1289 vs, 1175 vs, 1147 vs, 1105 s, 1079 vs, 847 w, 765 s, 679 w and 504 w cm^{-1}.

[Ni(PCAH)$_2$]·H$_2$O: $C_{26}H_{24}N_8NiO_3$ (555.3): calcd. C 56.24, H 4.36, N 20.18; found C 56.23, H 4.45, N 19.76. IR: $\tilde{\nu}_{max}$ = 3336 s, 3218 s, 1628 s, 1599 vs, 1552 w, 1485 vs, 1458 s, 1424 s, 1353 vs, 1339 vs, 1288 vs, 1174 vs, 1147 vs, 1107 s, 1083 vs, 847 w, 767 s, 679 w, 642 w and 504 w cm^{-1}.

[Cu(PCAH)$_2$]·H$_2$O: $C_{26}H_{24}CuN_8O_3$ (560.1): calcd. C 55.76, H 4.32, N 20.01; found C 55.61, H 4.40, N 19.63. IR: $\tilde{\nu}_{max}$ = 3329 s, 3212 s, 1628 w, 1598 vs, 1551 w, 1522 w, 1483 s, 1459 s, 1424 w, 1354 vs, 1337 vs, 1289 vs, 1174 vs, 1148 vs, 1104 s, 1075 s, 846 w, 766 s, 681 w, 622 w, and 505 w cm^{-1}.

[Zn(PCAH)$_2$]·H$_2$O: $C_{26}H_{24}N_8O_3Zn$ (561.9): calcd. C 55.58, H 4.30, N 19.94; found C 55.39, H 4.36, N 19.67. IR: $\tilde{\nu}_{max}$ = 3347 s, 3216 w, 1628 w, 1600 vs, 1553 w, 1521 w, 1487 s, 1460 s, 1426 w, 1354 vs, 1338 vs, 1289 vs, 1174 vs, 1147 vs, 1104 s, 1081 s, 851 w, 768 s, 680 w, 640 w and 504 w cm^{-1}. ^{1}H NMR ([D$_6$]DMSO): δ = 5.60 (s, 2 H), 6.50 (d, 2 H), 7.28 (m, 1 H), 7.64 (d, 1 H), 7.80 (d, 2 H), 7.91 (m, 2 H) and 8.55 (s, 1 H) ppm.

Crystals of [M(PCAH)$_2$]·H$_2$O (M = Mn, Ni, Cu, Zn) and [Cu(PCIH)$_2$]: The perchlorate salt of the respective metal (14 μmol) and the ligand (35 μmol; 1:2.5 ratio) were dissolved in 6 mL of MeCN/toluene (3:2) and 40 μL of Et_3N was added to the solution. The solutions were allowed to concentrate slowly and crystals suitable for X-ray work were formed. IR spectra of the crystals were found to be identical to the spectra of their respective counterparts in the bulk syntheses. Crystals of [Ni(PCIH)$_2$]·2H$_2$O were obtained from vapour diffusion of 2-propanol into a concentrated DMSO solution of the complex.

Trivalent and Oligomeric Complexes

[Co(PCIH)$_2$][CoCl$_3$]·2H$_2$O: HPCIH (0.5 g, 2 mmol) was dissolved in methanol (50 mL). $CoCl_2$·6H$_2$O (0.26 g, 1 mmol) was added to the solution and the mixture was refluxed for 16 h. Dichloromethane vapour diffusion into the concentrated reaction mixture afforded red-brown crystals suitable for X-ray work. Further crops were obtained from diethyl ether vapour diffusion into a concentrated methanolic solution of the solid. Total yield was 21%. $C_{24}H_{22}Cl_3Co_2N_8O_4$ (710.1): calcd. C 40.56, H 3.12, N 15.73; found C 40.45, H 3.02, N 15.87. IR: $\tilde{\nu}_{max}$ = 1618 s, 1484 vs, 1446 vs, 1380 vs, 1341 s, 1209 s, 1151 s, 1077 s, 848 w, 727 s and 606 s cm^{-1}.

[Co(HPCIH)(PCIH)](NO$_3$)$_2$·H$_2$O·0.5CH$_3$OH: HPCIH (0.5 g, 2 mmol) was dissolved in 50 mL of methanol. Co(NO$_3$)$_2$·6H$_2$O (0.32 g, 1.1 mmol) was added to the solution and the mixture gently refluxed for 16 h. A precipitate of the product formed on cooling and was collected and washed with diethyl ether. Diethyl ether vapour diffusion into a concentrated methanolic solution of the mother liquor afforded crystals suitable for X-ray work. More crystals were obtained from slow concentration of the mother liquor. Total yield was 16%. $C_{24.5}H_{23}CoN_{10}O_{9.5}$ (668.5): calcd. C 44.02, H 3.47, N 20.95; found C 44.10, H 3.40, N 21.07. IR: $\tilde{\nu}_{max}$ = 1636 s, 1540 s, 1483 s, 1448 vs, 1383 vs, 1208 s, 1148 s, 1078 s, 1000 w, 928 w, 844 w, 750 s, 716 s, 682 w and 607 w cm^{-1}.

[Co(HPCIH)$_2$](NO$_3$)$_3$·2H$_2$O: HPCIH (1.0 g, 4 mmol) was dissolved in 50 mL of methanol. Co(NO$_3$)$_2$·6H$_2$O (0.55 g, 2 mmol) was added to the solution and the mixture gently refluxed for 48 h. A precipitate of the product formed on cooling and was collected and washed with diethyl ether. Total yield was 81%. $C_{24}H_{26}CoN_{11}O_{13}$ (733.5): calcd. C 39.30, H 3.30, N 21.01; found C 39.36, H 2.94, N 21.02. IR: $\tilde{\nu}_{max}$ = 3063 s, 2526br, 1636 s, 1527 s, 1482 s, 1448 vs, 1384 vs, 1300 s, 1213 s, 1151 s, 1077 s, 1006 w, 930 w, 826 w, 749 s, 716 s, 682 w and 600 w cm^{-1}.

[Co(PCIH)$_2$]NO$_3$·2H$_2$O: Addition of 2 equiv. of Et_3N to an aqueous solution of [Co(HPCIH)$_2$](NO$_3$)$_3$·2H$_2$O resulted in immediate precipitation of the product, which was collected and washed with diethyl ether. Total yield was 75%. $C_{24}H_{22}CoN_9O_7$ (607.4): calcd. C 47.46, H 3.65, N 20.75; found C 47.52, H 3.42, N 20.73. IR: $\tilde{\nu}_{max}$ =1610 s, 1567 w, 1483 s, 1443 vs, 1384 vs, 1340 s, 1209 s, 1150 s, 1079 s, 927 w, 840 w, 780 w, 750 w, 713 s, and 607 w cm^{-1}.

[Co(PCAH)$_2$]Cl·4H$_2$O: HPCAH (0.5 g, 2 mmol) was dissolved in 50 mL of methanol. $CoCl_2$·6H$_2$O (0.23 g, 1 mmol) was added to the solution and the mixture was gently refluxed for 16 h. A red precipitate of the product formed on cooling. The solution was concentrated to approximately one third of the original volume and the precipitate collected and washed with cold methanol and then with distilled water. Total yield was 48%. $C_{26}H_{30}ClCoN_8O_6$ (645.0): calcd. C 48.42, H 4.69, N 17.37; found C 48.04, H 4.34, N 17.05. IR: $\tilde{\nu}_{max}$ = 3328 s, 3207 w, 1624 w, 1601 vs, 1559 w, 1522 w, 1479 s, 1451 s, 1374 vs, 1287 s, 1215 w, 1174 vs, 1148 s, 1079 s, 843 w, 758 w, 682 w, 636 w and 511 w cm^{-1}. ^{1}H NMR ([D$_6$]DMSO): δ = 6.14 (s, 2 H), 6.47 (d, 2 H), 7.39 (t, 1 H), 7.64 (d, 2 H), 7.85 (d, 1 H), 8.07 (m, 2 H) and 9.39 (s, 1 H). ^{13}C NMR ([D$_6$]DMSO): δ = 112.8, 116.2, 126.4, 127.7, 131.4, 141.8, 148.6, 151.6, 153.8, 160.7 and 184.0 ppm.

[{MnCl$_2$(DMSO)(HPCIH)}$_2$Mn(DMSO)$_2$Cl$_2$]: The preparation of [Mn(PCIH)$_2$] (described above) occasionally resulted in a product contaminated with small amounts of $MnCl_2$ as a co-precipitate. Dissolution of this crude compound in DMSO followed by vapour diffusion of 2-propanol into the mixture afforded yellow crystals suitable for X-ray work. [{MnCl$_2$(DMSO)(HPCIH)}$_2$Mn-

$(DMSO)_2Cl_2$]. $C_{32}H_{44}Cl_6Mn_3N_8O_6S_4$ (1142.5): calcd. C 33.64, H 3.88, N 9.81; found C 33.59, H 3.80, N 9.76.

[Zn(HPCIH)SO_4]·3.5H_2O: HPCIH (0.5 g, 2 mmol) was dissolved in 15 mL of methanol. Then $ZnSO_4·7H_2O$ (0.28 g, 1 mmol) was added to the solution and the mixture gently refluxed for 18 h. The mixture was cooled and a yellow precipitate of the product was collected and washed with diethyl ether. A small amount of the product was dissolved in minimum amount of acetonitrile/toluene (1:1) mixture. Slow concentration of the solution yielded crystals suitable for X-ray work. Total yield was 20%. $C_{12}H_{17}N_4O_{8.5}SZn$ (450.7): calcd. C 31.98, H 3.80, N 12.43; found C 32.10, H 3.60, N 12.37. IR: $\tilde{\nu}_{max}$ = 1684 vs, 1653 vs, 1575 vs, 1551 vs, 1472 s, 1433 s, 1406 s, 1361 s, 1298 vs, 1147 s, 1071 s, 926 s, 846 s, 781 s, 750 s and 686 vs cm^{-1}.

Crystallography: Cell constants were determined by a least-squares fit to the setting parameters of 25 independent reflections measured with an Enraf−Nonius CAD4 four-circle diffractometer employing graphite-monochromated Mo-K_α radiation. Data reduction, absorption correction (ψ-scans) and all calculations were performed with the WINGX suite of programs.[51] Structures were solved by direct methods for HPCAH, [Mn(PCAH)$_2$], [Ni(PCAH)$_2$], [Cu(PCAH)$_2$], [Zn(PCAH)$_2$] and [Cu(PCIH)$_2$] and Patterson methods for [Ni(PCIH)$_2$], [Co^{III}(PCIH)$_2$$Co^{II}Cl_3$] and [$Co^{III}$(HPCIH)(PCIH)]$NO_3$ with SHELXS,[52−54] and with SIR92 for [{$MnCl_2$(DMSO)(HPCIH)}$_2$Mn(DMSO)$_2$$Cl_2$] and [Zn(HPCIH)]$SO_4$.[55] Structures were refined by full-matrix least-squares analysis with SHELXL-97.[56] All non-H atoms were refined with anisotropic thermal parameters. Aryl and amino H-atoms were included at estimated positions whereas amide H-atoms (if any) were first located from difference maps then restrained in a similar manner to that employed for the remaining H-atoms. Crystal data appear in Tables 2 and 4 and selected bond lengths and angles are presented in Tables 3, Table 5 and 6. The atomic nomenclature is defined in Figures 2−8 and drawn with programs PLATON[57] and ORTEP-3.[58] CCDC-182551 to -182561 contain the supplementary crystallographic data for this paper. These data can be obtained free of charge at www.ccdc.cam.ac.uk/conts/retrieving.html [or from the Cambridge Crystallographic Data Centre, 12 Union Road, Cambridge CB2 1EZ, UK; Fax: (internat.) + 44-1223/336-033; E-mail: deposit@ccdc.cam.ac.uk].

Acknowledgments

P. C. thanks the Department of Chemistry, University of Queensland for a departmental scholarship. P. V. B. acknowledges financial support from the University of Queensland. D. R. thanks the National Health and Medical Research Council for grant and fellowship support. We also thank Mr. K. Thurecht for assistance with the EPR spectral measurements.

[1] J. B. Porter, E. R. Huehns, R. C. Hider, *Baillière's Clin. Haematol.* **1989**, *2*, 257.
[2] C. Hershko, *Baillière's Clin. Haematol.* **1994**, *7*, 965.
[3] Z. D. Liu, R. C. Hider, in *Molecular and Cellular Iron Transport* (Ed.: D. M. Templeton), Marcel Dekker, Inc., New York, **2001**, p. 321.
[4] D. R. Richardson, P. Ponka, *Am. J. Hematol.* **1998**, *58*, 299.
[5] N. F. Olivieri, G. M. Brittenham, *Blood* **1997**, *90*, 1161.
[6] N. F. Olivieri, G. M. Brittenham, *Blood* **1999**, *94*, 3302.
[7] G. J. Kontoghiorghes, Ph. D thesis, University of Essex, Colchester, **1982**.
[8] N. F. Olivieri, G. M. Brittenham, D. Matsui, M. Berkovitch, L. M. Blendis, R. G. Cameron, R. A. McClelland, P. P. Liu, D. M. Templeton, G. Koren, *N. Engl. J. Med.* **1995**, *332*, 918.
[9] F. N. al-Refaie, B. Wonke, A. V. Hoffbrand, *Eur. J. Hematol.* **1994**, *53*, 298.
[10] A. V. Hoffbrand, F. Al-Refaie, B. Davis, N. Siritanakatkul, B. F. A. Jackson, J. Cochrane, E. Prescott, B. Wonke, *Blood* **1998**, *91*, 295.
[11] N. F. Olivieri, G. M. Brittenham, C. E. McLaren, D. M. Templeton, R. G. Cameron, R. A. McClelland, A. D. Burt, K. A. Fleming, *N. Engl. J. Med.* **1998**, *339*, 417.
[12] D. R. Richardson, *J. Lab. Clin. Med.* **2001**, *137*, 324.
[13] L. J. Anderson, B. Wonke, E. Prescott, S. Holden, J. M. Walker, D. J. Pennell, *Lancet* **2002**, *360*, 516.
[14] D. R. Richardson, *Lancet* **2002**, *360*, 501.
[15] I. R. Wanless, G. Sweeney, A. P. Dhillon, M. Guido, A. Piga, R. Galanello, M. R. Gamberini, E. Schwartz, A. R. Cohen, *Blood* **2002**, *100*, 1566.
[16] Y. Aydinok, G. Nisli, K. Kavakli, C. Coker, M. Kantar, N. Centingul, *Acta Haematol.* **1999**, *102*, 17.
[17] G. Link, A. M. Konijn, W. Breuer, Z. I. Cabantchik, C. Hershko, *J. Lab. Clin. Med.* **2001**, *138*, 130.
[18] E. Becker, D. R. Richardson, *Int. J. Biochem. Cell Biol.* **2001**, *33*, 1.
[19] D. R. Richardson, C. Mouralian, P. Ponka, E. Becker, *Biochim. Biophys. Acta-Mol. Basis Dis.* **2001**, *1536*, 133.
[20] E. Becker, D. R. Richardson, *J. Lab. Clin. Med.* **1999**, *134*, 510.
[21] D. R. Richardson, E. Becker, P. V. Bernhardt, *Acta Crystallogr., Sect. C* **1999**, *55*, 2102.
[22] D. Richardson, P. V. Bernhardt, E. M. Becker, in *PCT Int. Appl.*, University of Queensland, Australia, Heart Research Institute Ltd., 0117530, **2001**, p. 50.
[23] P. V. Bernhardt, P. Chin, D. R. Richardson, *J. Biol. Inorg. Chem.* **2001**, *6*, 801.
[24] W. Kemp, in *Organic Spectroscopy*, 2nd ed., Macmillan Education Ltd, Hampshire, **1987**, p. 65.
[25] R. M. Silverstein, G. C. Bassler, T. C. Morrill, in *Spectrometric Identification of Organic Compounds*, 4th ed., John Wiley & Sons, Inc., **1981**, p. 124.
[26] L. El-Sayed, M. F. Iskander, *J. Inorg. Nucl. Chem.* **1971**, *33*, 435.
[27] A. V. Lakshmi, N. R. Sangeetha, S. Pal, *Indian J. Chem. Sect A* **1997**, *36*, 844.
[28] N. R. Sangeetha, S. Pal, *J. Coord. Chem.* **1997**, *42*, 157.
[29] J. W. Pyrz, A. L. Roe, L. J. Stern, L. Que, *J. Am. Chem. Soc.* **1985**, *107*, 614.
[30] R. N. Mukherjee, O. A. Rajan, A. Chakravorty, *Inorg. Chem.* **1982**, *21*, 785.
[31] R. J. P. Williams, *J. Chem. Soc.* **1955**, 137.
[32] S. Pal, G. V. Karunakar, N. R. Sangeetha, V. Susila, *J. Coord. Chem.* **2000**, *50*, 51.
[33] S. Pal, A. Choudhury, B. Geetha, N. R. Sangeetha, V. Kavita, V. Susila, *J. Coord. Chem.* **1999**, *48*, 87.
[34] H. Oshio, E. Ino, I. Mogi, T. Ito, *Inorg. Chem.* **1993**, *32*, 5697.
[35] M. H. Moore, L. R. Nassimbeni, M. L. Niven, *J. Chem. Soc., Dalton Trans.* **1987**, 2125.
[36] S. Seth, S. Chakraborty, *Acta Crystallogr., Sect. C* **1984**, *C40*, 1530.
[37] A. Seal, S. Ray, *Acta Crystallogr., Sect. C* **1984**, *C40*, 929.
[38] N. R. Sangeetha, C. K. Pal, P. Ghosh, S. Pal, *J. Chem. Soc., Dalton Trans.* **1996**, 3293.
[39] A. Mangia, M. Nardelli, C. Pelizzi, G. Pelizzi, *J. Chem. Soc., Dalton Trans.* **1973**, 1141.
[40] S. Dutta, V. Manivannan, L. G. Babu, S. Pal, *Acta Crystallogr., Sect. C* **1995**, *51*, 813.
[41] M. R. Maurya, D. C. Antony, S. Gopinathan, V. G. Puranik, S. S. Tavale, C. Gopinathan, *Bull. Chem. Soc. Jpn.* **1995**, *68*, 2847.
[42] X. M. Zhang, X. Z. You, X. Wang, *Polyhedron* **1996**, *15*, 1793.
[43] W. Wang, F. L. Zeng, X. Wang, M. Y. Tan, *Polyhedron* **1996**, *15*, 1699.
[44] S. P. Rath, S. Mondal, A. Chakravorty, *Inorg. Chim. Acta* **1997**, *263*, 247.
[45] N. R. Sangeetha, K. Baradi, R. Gupta, C. K. Pal, V. Manivannan, S. Pal, *Polyhedron* **1999**, *18*, 1425.

[46] F. A. Cotton, G. Wilkinson, C. A. Murillo, M. Bochmann, in *Advanced Inorganic Chemistry*, 6th ed., John Wiley & Sons, Inc., **1999**, p. 865.
[47] A. E. Martell, R. M. Smith, R. J. Motekaitis, *Critically selected stability constants of metal complexes database*, 4th ed., Texas A & M University, **1997**.
[48] R. A. Martinelli, G. R. Hanson, J. S. Thompson, B. Holmquist, J. R. Pilbrow, D. S. Auld, B. L. Vallee, *Biochemistry* **1989**, *28*, 2251.
[49] P. Gans, A. Sabatini, A. Vacca, *J. Chem. Soc., Dalton Trans.* **1985**, 1195.
[50] S. G. Komurcu, S. Rollas, M. Ulgen, J. W. Gorrod, A. Cevikbas, *Boll. Chim. Farmac.* **1995**, *134*, 375.
[51] L. J. Farrugia, *J. Appl. Crystallogr.* **1999**, *32*, 837.
[52] G. M. Sheldrick, University of Göttingen, Germany, **1997**.
[53] G. M. Sheldrick, *Acta Crystallogr., Sect. A* **1990**, *46*, 467.
[54] G. M. Sheldrick, Z. Dauter, K. S. Wilson, H. Hope, L. C. Sieker, *Acta Crystallogr. Sect D* **1993**, *49*, 18.
[55] A. Altomare, G. Cascarano, C. Giacovazzo, A. Gualardi, *J. Appl. Crystallogr.* **1993**, *26*, 343.
[56] G. M. Sheldrick, University of Göttingen, Germany, **1997**.
[57] A. L. Spek, *Acta Crystallogr., Sect. A* **1990**, *46*, C34.
[58] L. J. Farrugia, *J. Appl. Crystallogr.* **1997**, *30*, 565.

Received July 10, 2002
[I02376]